

Crossover behavior of the crystal structure and the relation to magnetism in perovskite $RTiO_3$

K. Takubo,¹ M. Shimuta,¹ J. E. Kim,² K. Kato,^{2,3} M. Takata,^{2,3} and T. Katsufuji^{1,4,5}

¹Department of Physics, Waseda University, Tokyo 169-8555, Japan

²Japan Synchrotron Radiation Research Institute, Hyogo 679-5198, Japan

³RIKEN SPring-8 Center, Hyogo 679-5148, Japan

⁴Kagami Memorial Laboratory for Material Science and Technology, Waseda University, Tokyo 169-0051, Japan

⁵PRESTO, Japan Science and Technology Corporation, Saitama 332-0012, Japan

(Received 14 April 2010; revised manuscript received 25 May 2010; published 6 July 2010)

We found that a crossover behavior of the crystal structure at high temperatures dominates the magnetic state at low temperatures in the series of $RTiO_3$ (R is rare earth). At the crossover temperature, which exist only in the samples that become antiferromagnetic at lower temperatures, the temperature derivative of lattice constants changes its sign, and the crossover temperature approaches zero as the Neel temperature approaches zero in the phase diagram of the ionic radius of R vs temperature. This result indicates that the orbital state of the Ti ion dominates the low-temperature magnetic state in $RTiO_3$.

DOI: [10.1103/PhysRevB.82.020401](https://doi.org/10.1103/PhysRevB.82.020401)

PACS number(s): 75.25.Dk, 61.50.Ks, 75.30.Kz

A change in magnetic states in a series of compounds associated with a change in orbital states is a characteristic behavior in transition-metal oxides. A typical example is seen in doped perovskite manganites, $R_{1-x}A_xMnO_3$ (R is a rare earth and A an alkaline-earth ion). In this series of compounds, the ordering of Mn spins changes from ferromagnetism (FM) to A-type (ferromagnetic alignment of spins along planes), C-type (ferromagnetic along straight lines), G-type (conventional antiferromagnetic alignment), and CE-type (ferromagnetic along zigzag lines) antiferromagnetism (AFM) associated with the change of the Mn orbital ordering, which is induced by the variation in the hole concentration x and the average ionic radius of $R_{1-x}A_x$.¹ Another example is seen in (undoped) perovskite vanadates, RVO_3 , in which the ordering of V spins changes from C-type to G-type AFM associated with the change in the V orbital ordering from G-type to C-type.² In both cases, Kanamori-Goodenough-type discussion³⁻⁵ is applicable to explain the magnetic state on a specific type of orbital ordering.

On the other hand, the change in magnetic states in perovskite $RTiO_3$ with the change of rare earth (R) has not been fully understood yet. In this series of compounds, the ordering of Ti spins changes from G-type AFM with a larger ionic radius of R to FM with a smaller ionic radius of R , and the threshold is between $R=Sm$ (AFM) and Gd (FM).⁶⁻⁸ Various theoretical studies⁹⁻¹¹ indicate that there is antiferro-orbital ordering in the FM state, and NMR measurement,¹² polarized neutron scattering,¹³ and resonant x-ray scattering¹⁴ have confirmed the existence of such antiferro-orbital ordering, i.e., the alternate occupation of $\alpha|d_{xy}\rangle + \beta|d_{yz}\rangle$ and $\alpha|d_{xy}\rangle + \beta|d_{zx}\rangle$ orbitals in the Ti ion. However, the result of resonant x-ray scattering does not support the change in the orbital state associated with the change in the magnetic state from FM to AFM but indicates that the antiferro-orbital ordering seemingly survives even in the AFM state.¹⁵ Theoretically, it was proposed that the magnetic state changes from FM to AFM with a continuous variation of parameters but without a distinct change of orbital ordering.^{16,17}

Another experimental result related to the change in magnetic states in $RTiO_3$ is a variation in the crystal structure clarified by diffraction measurements.^{18,19} Namely, the ratio

of the a lattice constant to the b lattice constant of the orthorhombic $RTiO_3$ (with the so-called $GdFeO_3$ -type distortion), a/b , varies from $a/b < 1$ for the FM compounds to $a/b > 1$ for the AFM compounds. Microscopically, the ratio of the in-plane oxygen-oxygen bond along the a and b direction, $r_{O-O} = (O2-O2)_a / (O2-O2)_b$ ($O2$ refers to the in-plane oxygen) varies from $r_{O-O} \sim 1$ for the FM compounds to $r_{O-O} > 1$ for the AFM compounds, and the ratio of the two in-plane Ti-O bonds, $r_{Ti-O} = (Ti-O2)_{long} / (Ti-O2)_{short}$ varies from $r_{Ti-O} > 1$ for the FM to $r_{Ti-O} \sim 1$ for the AF compounds. This variation in bond length is consistent with the theoretical studies that the lattice distortion $r_{Ti-O} > 1$ favors the antiferro-orbital ordering and ferromagnetic ordering whereas $r_{O-O} > 1$ induces a trigonal crystal field to the t_{2g} orbital and favors the ferro-orbital ordering (where the $|a_{1g}\rangle = (|d_{xy}\rangle + |d_{yz}\rangle + |d_{zx}\rangle) / \sqrt{3}$ states extending toward the $\langle 111 \rangle$ direction are occupied) and antiferromagnetic ordering.²⁰ However, it is not obvious whether this type of lattice distortion exists *ab initio* and affects the orbital state of Ti or occurs as a result of orbital ordering.

One of the problems here is that both types of distortions (the variations of r_{O-O} and r_{Ti-O}) and both ferro-orbital and antiferro-orbital ordering do not violate the symmetry of the $GdFeO_3$ distortion (space group $Pbnm$), which is a common distortion observed in the compounds with a perovskite structure (even without transition metals). This makes the transition between two different orbital states unclear unlike the orbital ordering in manganites and vanadates that is accompanied with a clear change in the space group.

In this Rapid Communication, we studied the detailed temperature dependence of the crystal structure for $RTiO_3$ over a wide temperature range. We found that at very high temperatures ($T > 600$ K), the crystal structure varies with T in the same direction, i.e., $da/dT > 0$ and $db/dT < 0$, for all the samples but there exist crossover temperatures, T_s^* , only for the samples showing the AF state at low T and below T_s^* , the crystal structure behaves in such a way that $da/dT < 0$ and $db/dT > 0$. This result indicates that the crossover line of the crystal structure at high T dominates the magnetic-phase boundary at low T . We propose that this crossover arises

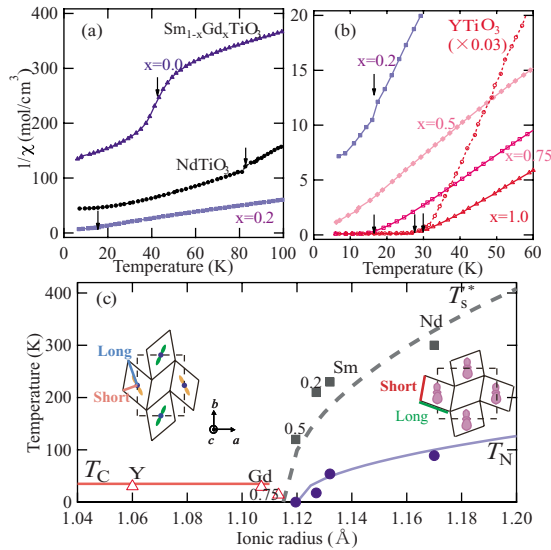


FIG. 1. (Color online) [(a) and (b)] Temperature dependence of inverse magnetic susceptibility $1/\chi(T)$ for $RTiO_3$. Arrows show (a) Neel temperatures (T_N) or (b) Curie temperatures (T_C). (c) Phase diagram of perovskite titanates. The solid lines correspond to magnetic ordering temperatures and the thick dashed line to the crossover in the structural change (see text).

from the orbital ordering and it becomes crossover because the $GdFeO_3$ -type lattice distortion acts as a “magnetic field” for the orbital degrees of freedom as pseudospins.

Single crystals of $RTiO_3$ with $R = Nd, Sm, Gd, Y$, and the mixed compounds, $Sm_{1-x}Gd_xTiO_3$ ($x = 0.2, 0.5, 0.75$) were grown by a floating zone method. X-ray diffraction measurement using a synchrotron radiation x-ray source was performed at SPring-8 BL02B2 equipped with a large Debye-Sherrer camera.²¹ For the measurement, single crystals were crushed into powder and then a precipitation method²² was applied to obtain fine powder with a homogeneous size. The powder was sealed in a 0.2 mm ϕ quartz capillary and temperature was controlled by a N_2 gas flow system between 90 and 800 K. Rietveld analysis of the diffraction data was performed with Rietan-2000.²³ Strain measurement by a strain-gauge technique was conducted for several samples between 20 and 300 K. For the measurement, the orientation of the single crystals was determined by a Laue method. Magnetic susceptibility was measured by a superconducting quantum interference device magnetometer.

Figures 1(a) and 1(b) show the result of (inverse) magnetic susceptibility and the magnetic-phase diagram. The ground state changes from FM to AFM in $Sm_{1-x}Gd_xTiO_3$ at $x = 0.5$. This result is consistent with the previous literature.^{6–8}

Figures 2(a)–2(c) show the variation of the a , b , and c lattice constants with temperature, in which the y axis is defined as $(\Delta L/L)_a = [a(T) - a(700 \text{ K})]/a(700 \text{ K})$, etc. Here, the T dependence of strain measured by a strain gauge, which is normalized to the value at 200 K obtained by the x-ray diffraction measurement, was also plotted in the same graphs. With decreasing T from 700 K, $(\Delta L/L)_a$ decreases for all the samples down to 400 K. However, at lower T , $(\Delta L/L)_a$ of some samples exhibits an upturn and increases

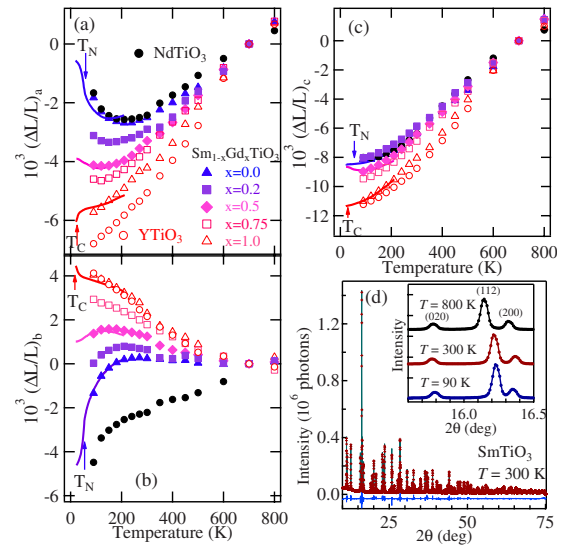


FIG. 2. (Color online) Variation in the (a) a , (b) b , and (c) c lattice constants with temperature. The y axes are defined as $\Delta L/L = [a(T) - a(700 \text{ K})]/a(700 \text{ K})$, etc. Symbols are the data obtained from x-ray diffraction measurement and solid lines are from strain measurement. (d) Synchrotron x-ray powder diffraction patterns (plus marks) and Rietveld refinement patterns (solid lines) of $SmTiO_3$ at 300 K with $\lambda = 0.7776 \text{ \AA}$. The solid line at the bottom corresponds to the difference between observed and calculated intensities. The inset shows the variation in the diffraction peaks, 020, 112, and 200 with temperature.

with decreasing T . By comparing the results with the magnetic-phase diagram shown in Fig. 1(c), it is found that the samples showing an upturn in $(\Delta L/L)_a$ are those showing the AF phase at low T . Furthermore, another anomaly exists at the magnetic-phase transition temperature in the data measured by a strain gauge; $(\Delta L/L)_a$ further increases below T_N for $SmTiO_3$ but decreases below T_C for $GdTiO_3$, consistent with the data previously reported.^{18,19,24} Therefore, the a lattice constant keeps on decreasing with decreasing T for the FM samples and further decreases at T_C whereas for the AFM samples, it first decreases with decreasing T but exhibits an upturn at a certain temperature and increases with decreasing T and further increases below T_N .

The behavior of $(\Delta L/L)_b$ is similar to $(\Delta L/L)_a$ but in the opposite direction. Namely, for the FM samples, the b lattice constant keeps on increasing with decreasing T and further increases at T_C whereas for the AFM samples, it first increases (or almost T independent) but exhibits a downturn at a certain temperature, and further decreases below T_N . On the other hand, the $(\Delta L/L)_c$ does not exhibit such a R -dependent behavior; c monotonically decreases with decreasing T for all the samples.

To see the characteristics in the T dependence of the lattice constants for $RTiO_3$ more clearly, the ratio of a to b , each of which is normalized to the value at 700 K, is plotted as a function of T in Fig. 3. As can be seen, a/b keeps on decreasing with decreasing T for $YTiO_3$, $GdTiO_3$, and $Sm_{1-x}Gd_xTiO_3$ with $x = 0.75$, all of which become FM at low T . However, an upturn of a/b appears for $Sm_{1-x}Gd_xTiO_3$ with $x = 0.5$, which is located at the magnetic phase boundary

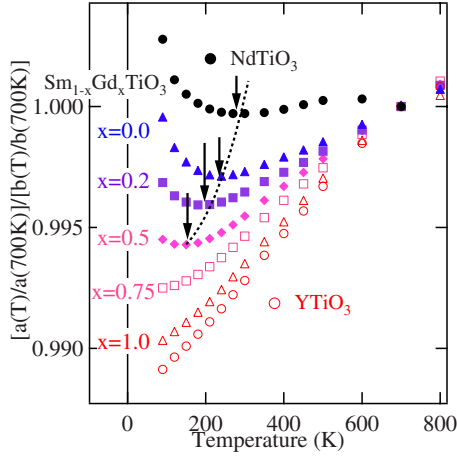


FIG. 3. (Color online) The ratio of the a lattice constant to the b lattice constant (normalized to the value at 700 K) as a function of temperature. Arrows show the minimum of the data (T_s^*) for each sample.

between the FM and AFM phases, and the temperature where the upturn occurs (the minimum of a/b shown by arrows) increases with decreasing x for $\text{Sm}_{1-x}\text{Gd}_x\text{TiO}_3$, and amounts to ~ 300 K for NdTiO_3 , all of which become AFM at low T .

The temperature where a/b shows a minimum, T_s^* , is plotted as a function of the ionic radius of R in Fig. 1(c), together with T_C and T_N . Note that T_s^* is not a transition temperature but should be regarded as a crossover temperature. As can be seen, T_s^* exist only on the AFM side. In other words, the crossover line for the crystal structure divides the FM and AFM phase at low T . This feature in the phase diagram indicates that T_s^* , a crossover temperature of the lattice, and T_N are correlated with each other.

To understand the microscopic nature of the crossover, we focus on the variation of bond lengths with temperature obtained by the Rietveld analysis. An example of the analysis is shown in Fig. 2(d).²⁰ In Fig. 4, $r_{\text{O-O}} = (\text{O2-O2})_a / (\text{O2-O2})_b$, which is coupled with the ferro-orbital ordering, and $r_{\text{Ti-O}} = (\text{Ti-O})_{\text{long}} / (\text{Ti-O})_{\text{short}}$, which is coupled with the antiferro-orbital ordering, are plotted as a function of T . As can be seen, $r_{\text{O-O}}$ exhibits a clear T dependence correlated with the T dependence of the lattice constants shown in Figs. 2 and 3; $r_{\text{O-O}}$ is larger than unity and becomes larger with

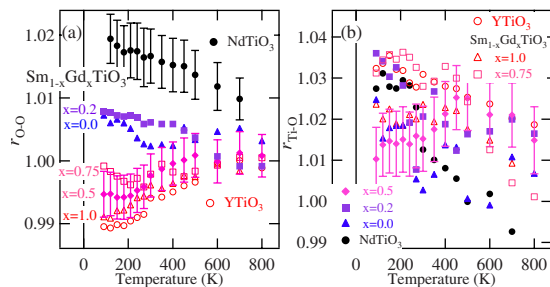


FIG. 4. (Color online) (a) The ratio of the two in-plane O-O bond lengths, $r_{\text{O-O}} = (\text{O2-O2})_a / (\text{O2-O2})_b$ and (b) the ratio of the two in-plane Ti-O bond lengths, $r_{\text{Ti-O}} = (\text{Ti-O})_{\text{long}} / (\text{Ti-O})_{\text{short}}$ as a function of temperature.

decreasing T for the AFM samples whereas $r_{\text{O-O}}$ keeps on decreasing with decreasing T for the FM samples. On the other hand, $r_{\text{Ti-O}}$ does not show a systematic T dependence. Theoretically, the deviation of $r_{\text{O-O}}$ from unity corresponds to a trigonal distortion of the TiO_6 octahedra, which favors the $|a_{1g}\rangle = (|d_{xy}\rangle + |d_{yz}\rangle + |d_{zx}\rangle) / \sqrt{3}$ orbital along the $\langle 111 \rangle$ direction and induces ferro-orbital ordering in the crystal.^{16,17} Inversely, the ferro-orbital ordering, in which an electron occupy the a_{1g} orbital at all the sites, induces a trigonal distortion of TiO_6 octahedra to further stabilize the orbital state. Thus, it can be concluded that in the AF samples, the ferro-orbital ordering occurs and that induces the trigonal distortion of TiO_6 octahedra and the deviation of $r_{\text{O-O}}$ from unity. This result means that the crossover line in Fig. 1(c) corresponds to a crossover from the high- T phase, which is likely to be the antiferro-orbital state, to the low- T phase, the ferro-orbital state.

As discussed in the introduction both the ferro-orbital ordering with the occupancy of the $|a_{1g}\rangle = (|d_{xy}\rangle + |d_{yz}\rangle + |d_{zx}\rangle) / \sqrt{3}$ state and the antiferro-orbital ordering with the alternate occupancy of $\alpha|d_{xy}\rangle + \beta|d_{yz}\rangle$ and $\alpha|d_{xy}\rangle + \beta|d_{zx}\rangle$ states do not violate the symmetry of the GdFeO_3 distortion. In this situation, the ferro-orbital state and the antiferro-orbital state cannot be eigenstates but they are mixed. Namely, the GdFeO_3 distortion inherently existing in the crystal acts as a “magnetic” field to the orbital degrees of freedom as pseudospins. Thus, it is reasonable that orbital ordering (pseudospin ordering) becomes crossover under the influence of a lattice distortion (an applied magnetic field), similar to the situation in the ferromagnetic spin system that loses its critical behavior with applied magnetic field.

It should be noted that the $h00$ and $00l$ peaks with the odd number of h, l in the resonant x-ray scattering, whose existence has been interpreted as the antiferro-orbital ordering, appear unless the occupancy of the $|d_{yz}\rangle$ and $|d_{zx}\rangle$ is completely the same in RTiO_3 . In other words, with the existence of the GdFeO_3 distortion, the appearance of these peak does not necessarily mean the antiferro-orbital ordering. The present experimental result indicates that the ferro- or antiferro-orbital ordering manifest itself in the temperature dependence of some parameters, $r_{\text{O-O}}$ in this case. We speculate that the study of the detailed temperature dependence in the intensity of the resonant x-ray scattering will give more direct evidence on this issue.

One of the important aspects in the present experimental result is that the antiferro-orbital ordering is the higher- T phase and the ferro-orbital ordering is the lower- T phase. This seems inconsistent with the model proposed by Mochizuki and Imada,^{16,17} where the ferro-orbital ordering is stabilized by the trigonal distortion and the crystal field inherently existing in the crystal. In the language of spin systems, this can be described in such a way that the AFM state would be the ground state without a magnetic field but the FM state is stabilized by a magnetic field. In this case, it never happens in spin systems that the AFM state, which is stabilized by a spin-spin interaction, is the high- T phase and the FM state, which is stabilized by a magnetic field, is the low- T phase. The difference of the present orbital system from the spin systems is that a magnetic field, corresponding to a lattice distortion as a real quantity, is also affected by the pseu-

dospin ordering, i.e., orbital ordering. Therefore, both the ordering of the t_{2g} states in Ti and the lattice distortion, particularly a trigonal distortion of TiO_6 octahedra, have to be taken into account simultaneously to understand the phase diagram of RTiO_3 .

In summary, we studied the crystal structure of RTiO_3 over a wide temperature range (80–800 K) with various rare-earth ions R across the boundary of the AFM and FM phases. We found crossover temperatures T_s^* existing only in the samples that become antiferromagnetic at lower temperatures, where the temperature dependence of the lattice constants changes its sign. Microscopically, the ratio of the in-plane oxygen-oxygen bond along the a and b directions, $r_{\text{O-O}} = (\text{O2-O2})_a / (\text{O2-O2})_b$, deviates from unity ($r_{\text{O-O}} > 1$) below T_s^* , resulting in the enhancement of the trigonal distortion

of TiO_6 that favors the occupancy of the nondegenerate state, $|a_{1g}\rangle = (|d_{xy}\rangle + |d_{yz}\rangle + |d_{zx}\rangle) / \sqrt{3}$. The present results indicate that the variation in magnetic states from the AFM to FM in the series of RTiO_3 is dominated by the variation in orbital states occurring at higher temperatures.

We thank H. Sawa and E. Nishibori for fruitful discussions. This work was partly supported by Grant-in-Aids for Scientific Research on Priority Areas (Grant No. 20046014) from MEXT and Scientific Research B (Grant No. 19340102) from JSPS of Japan. The synchrotron-radiation experiments were performed at the BL02B2 in the SPring-8 with the approval of the Japan Synchrotron Radiation Research Institute (JASRI) (Proposal No. 2007B1158).

-
- ¹Y. Tokura and N. Nagaosa, *Science* **288**, 462 (2000) and references therein.
- ²S. Miyasaka, Y. Okimoto, M. Iwama, and Y. Tokura, *Phys. Rev. B* **68**, 100406(R) (2003).
- ³J. B. Goodenough, *Phys. Rev.* **100**, 564 (1955).
- ⁴J. Kanamori, *J. Phys. Chem. Solids* **10**, 87 (1959).
- ⁵K. I. Kugel and D. I. Khomskii, *Zh. Eksp. Teor. Fiz.* **64**, 369 (1973) [*Sov. Phys. JETP* **37**, 725 (1973)].
- ⁶J. E. Greedan, *J. Less-Common Met.* **111**, 335 (1985).
- ⁷G. Amow, J.-S. Zhou, and J. B. Goodenough, *J. Solid State Chem.* **154**, 619 (2000).
- ⁸G. Amow, J. E. Greedan, and C. Ritter, *J. Solid State Chem.* **141**, 262 (1998).
- ⁹M. Mochizuki and M. Imada, *New J. Phys.* **6**, 154 (2004).
- ¹⁰E. Pavarini, A. Yamasaki, J. Nuss, and O. K. Andersen, *New J. Phys.* **7**, 188 (2005).
- ¹¹I. V. Solovyev, *Phys. Rev. B* **69**, 134403 (2004).
- ¹²M. Itoh, M. Tsuchiya, H. Tanaka, and K. Motoya, *J. Phys. Soc. Jpn.* **68**, 2783 (1999).
- ¹³J. Akimitsu, H. Ichikawa, N. Eguchi, T. Miyano, M. Nishi, and K. Kakurai, *J. Phys. Soc. Jpn.* **70**, 3475 (2001).
- ¹⁴H. Nakao, Y. Wakabayashi, T. Kiyama, Y. Murakami, M. v. Zimmermann, J. P. Hill, D. Gibbs, S. Ishihara, Y. Taguchi, and Y. Tokura, *Phys. Rev. B* **66**, 184419 (2002).
- ¹⁵M. Kubota, H. Nakao, Y. Murakami, Y. Taguchi, M. Iwama, and Y. Tokura, *Phys. Rev. B* **70**, 245125 (2004).
- ¹⁶M. Mochizuki and M. Imada, *J. Phys. Soc. Jpn.* **70**, 2872 (2001).
- ¹⁷M. Mochizuki and M. Imada, *Phys. Rev. Lett.* **91**, 167203 (2003).
- ¹⁸M. Cwik, T. Lorenz, J. Baier, R. Müller, G. André, F. Bourée, F. Lichtenberg, A. Freimuth, R. Schmitz, E. Müller-Hartmann, and M. Braden, *Phys. Rev. B* **68**, 060401(R) (2003).
- ¹⁹A. C. Komarek, H. Roth, M. Cwik, W. D. Stein, J. Baier, M. Kriener, F. Bourée, T. Lorenz, and M. Braden, *Phys. Rev. B* **75**, 224402 (2007).
- ²⁰See supplementary material at <http://link.aps.org/supplemental/10.1103/PhysRevB.82.020401> for the detailed discussion on the orbital states and crystal structure.
- ²¹E. Nishibori, M. Takata, K. Kato, M. Sakata, Y. Kubota, S. Aoyagi, Y. Kuroiwa, M. Yamakata, and N. Ikeda, *Nucl. Instrum. Methods Phys. Res. A* **467-468**, 1045 (2001).
- ²²M. Takata, E. Nishibori, K. Kato, M. Sakata, and Y. Moritomo, *J. Phys. Soc. Jpn.* **68**, 2190 (1999).
- ²³F. Izumi and T. Ikeda, *Mater. Sci. Forum* **321-324**, 198 (2000).
- ²⁴J. Hemberger, H.-A. Krug von Nidda, V. Fritsch, J. Deisenhofer, S. Lobina, T. Rudolf, P. Lunkenheimer, F. Lichtenberg, A. Loidl, D. Bruns, and B. Büchner, *Phys. Rev. Lett.* **91**, 066403 (2003).